Modulated surface texturing of temporary Al foils substrates for high-efficiency thin-film, flexible solar cells

Limodio, Gianluca; Bartesaghi, Davide; Hietkamp, Maurice; Rajagopal, Devika; Nawaratne, Sajith; Hamers, Edward; Smets, Arno

DOI
10.1109/PVSC45281.2020.9300722

Publication date
2020

Document Version
Accepted author manuscript

Published in
2020 47th IEEE Photovoltaic Specialists Conference, PVSC 2020

Modulated surface texturing of temporary Al foils substrates for high-efficiency thin-film, flexible solar cells

Gianluca Limodio
PVMD group
Delft University of Technology
Delft, The Netherlands
g.limodio@tudelft.nl

Davide Bartesaghi
HyET Solar B.V
Arnhem, The Netherlands
davide.bartesaghi@hyetsolar.com

Maurice Hietkamp
HyET Solar B.V
Arnhem, The Netherlands
m.hietkamp@outlook.com

Devika Rajagopal
PVMD group
Delft University of Technology
Delft, The Netherlands
D.Rajagopal@student.tudelft.nl

Sajith Nawaratne
PVMD group
Delft University of Technology
Delft, The Netherlands
S.B.Nawaratne@student.tudelft.nl

Edward Hamers
HyET Solar B.V
Arnhem, The Netherlands
edward.hamers@hyetsolar.com

Arno Smets
PVMD group
Delft University of Technology
Delft, The Netherlands
A.H.M.Smets@tudelft.nl

***Abstract* — In this work we focus on texturing Al substrate in order to employ the modulated surface texturing approach for thin-film, flexible, micromorph solar cells. We deployed two different methods to induce micro-craters in Al foil, i) bare Al etching by KOH and ii) AZO sacrificial layer etched in KOH. After modelling the etching kinetics of KOH on Al, we characterized the 2D correlation length and rms roughness of these samples and find the optimal aspect ratio of ~12% to deposit high-quality 3 µm-thick nc-Si. Finally, excellent angular scattering properties have been measured for both employed methods.**

Keywords—thin-film solar cells, flexible, Al substrate, etching

I. Introduction

In thin-film, flexible solar cells it is of primary importance to maximize absorption of photons within the photoactive absorber layer [1]. In single junction solar cells, the light trapping is employed by using a nano-textured substrate via TCO [2][3][4]. In multi-junction solar cells, the light trapping schemes have to comply with high quality and thick absorber layers to ensure high open-circuit voltage (V_{OC}) [5]. Indeed, a lower V_{OC} is observed when the introduction of textured interface leads to defect-rich absorber layers [6][7][8][9]. For this reason, advanced light trapping scheme must be employed in the case of multi-junction solar cells. This scheme should be capable to both enhance light trapping and allow high-quality PV materials during solar cells fabrication. These limitations are overcome by the so-called modulated surface texturing (MST) approach. It consists of superimposing the micro-sized craters induced on the substrate with naturally nano-texturing of a TCO [10]. This light trapping scheme has proven to be very effective in silicon-based thin-film solar cells on glass substrates, with initial efficiency of 14.5% and a stabilized efficiency of 12.5% on micromorph tandem device [11] close to the world record of 12.7% [12]. Roll-to-roll (R2R) processed PowerFoil® [13] is an unique concept in which lightweight flexible thin-film silicon solar cells are processed on temporary aluminum foils. After interconnection and back encapsulation, the temporary Al substrate is replaced by a transparent encapsulation foil. In this work, we employ the MST approach on temporary Al foils for thin-film, silicon-based, flexible solar cells. The MST will facilitate better light trapping and processing of high quality nanocrystalline silicon bottom cell (without defect-rich filaments) with higher V_{OC} values. The objective is to form large micro-craters in the Al foil substrate. These craters will be superimposed by naturally nano-textured TCO. Then, the front TCO and micromorph solar cell will be deposited in a R2R process. After encapsulation and back contact deposition, the Al foil will be finally removed [14], leaving MST structure imprinted on the surface of the solar cell. Figure 1 shows a BIPV application of thin-film solar cells based on this production process.

Figure 1 BIPV application of HyEt thin-film solar cells.

II. Experimental details

The starting material is a 107 µm-thick Al foil pure at 99% grade. Before processing the foils, they are cleaned in acetone and isopropanol ultra-sonic bath. After every etching treatment, Al foils are treated in 1% H_3PO_4 diluted in water to remove solid residuals.

A. Bare Al anisotropic etching

For this set of experiments, foils are etched in a solution of KOH:H_20 at varying concentration from 2% to 10%. Temperature of the solution is varied from 35 °C to 70 °C. Etching time is varied from 1 to 4 minutes.

B. Etching of a transparent conductive oxide sacrificial layer

By employing this approach, an AZO sacrificial layer (~ 600 nm-thick deposited at 300 °C with a power of 300 W) is deposited and it is subsequently etched in 10% KOH:H_20 at different temperatures between 35 and 70 °C. The etching time is sufficient to etch the AZO layer completely. The rationale is that the pinholes contained in this sacrificial layer are a catalyst for an anisotropic etching. The approach is similar to the one employed on glass substrates in Ref. [11].

C. Characterization

The etched samples are characterized by Philips XL50 scanning electron microscopy (SEM) and by atomic force Microscopy (AFM). After data post-processing, correlation length (L_C) and the root mean square roughness (σ_{rms}) are evaluated. In order to evaluate the quality of angular scattering of light of the etched substrate, the angular intensity diffraction (AID) is measured by a spectrophotometer.

III. Results and Discussion

A. KOH etching

Firstly, in order to evaluate the possibility of employing KOH etching in a R2R process, we map the foil thickness after etching with respect to KOH concentration, etching temperature and time. Temperature samples are 35, 50 and 70 °C, while concentration samples are 20, 40, 60, 80 and 100 g/L.

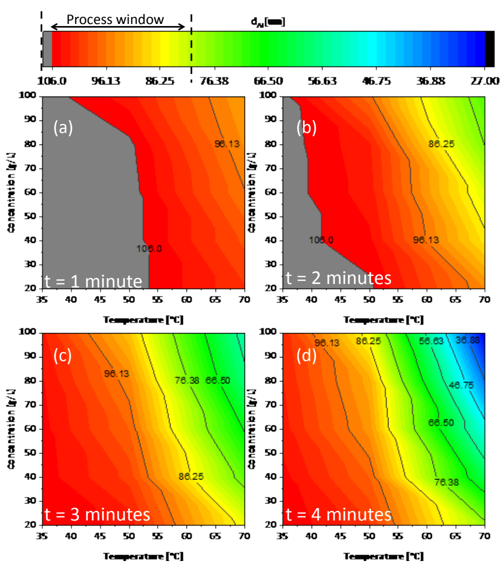

Figure 2 Etching map of KOH etching of Al foils depending on temperature and KOH concentration at different etching times. A scale is depicted with indication of the process window for R2R process.

Figures 2 show the map of Al foil thickness by varying etching temperature, concentration and time. As expected, short time (Figures (a) and (b)) have almost no impact when low temperature (T = 35 °C) is employed. For longer time (Figure 2 (c) and (d)), even at low temperature, ~5 µm of Al is etched. For high temperature (T = 70 °C), already short etching time (1 and 2 minutes) etches more than 10 µm of Al. If we etch it for longer time (3 and 4 minutes), most of the foil is etched away and it is not compatible anymore with R2R processing. From this map, we calculated the etching rate for different KOH concentration shown in the Arrhenius plot in figure 3.

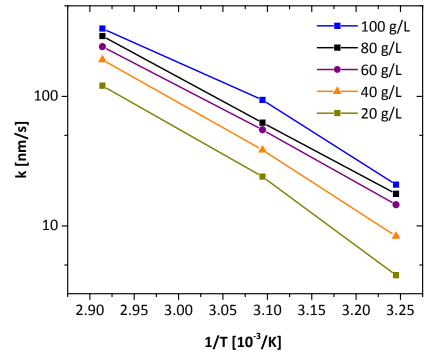

Figure 3 Arrhenius plot of the KOH etch rate for various concentrations

By fitting these Arrhenius plots, we obtain activation energy and pre-exponential factor to understand the kinetics of the etching process. Table 1 illustrates these values. Activation energy is found close to values calculated for silicon in [15][16], while the pre-exponential factor is significantly lower. This would suggest that the KOH etching on Al foil is less effective than on silicon wafers.

Table 1 Activation energy and pre-exponential factor for different KOH concentration

KOH [g/L]	20	40	60	80	100
E_a[eV]	0.60	0.57	0.50	0.50	0.50
A[10^6 nm/s]	3.00	1.50	0.50	0.52	0.51

To look at the shape of these KOH-etched Al foils, we took SEM images shown in figure 4. This etching is employed at 70 °C for 2 minutes with concentration increasing from 60 to 100 g/L. It is clear how the craters' size increases.

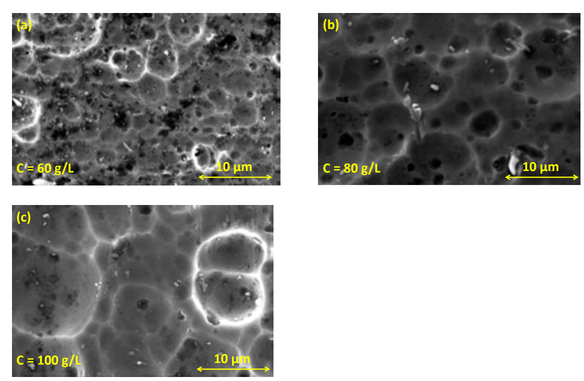

Figure 4 SEM of KOH-etched Al foil at T = 70 °C for t = 2 minutes, with KOH concentration of; (a) 60 g/L, (b) 80 g/L, (c) 100 g/L.

By employing AFM on these samples, we find out the correlati on length and rms roughness displayed in table 2.

Table 2 Parameters of KOH-etched at different KOH concentration

Sample	c [g/L]	L_c [µm]	σ_{RMS} [nm]	Lc/σ_{RMS}
1	60	3.398	416	0.122
2	80	3.804	470	0.123
3	100	4.044	472	0.117

Both correlation length and rms roughness increase with KOH concentration such that aspect ratio is in the range of ~12%. It has already been shown how this aspect ratio is the optimal to grow 3 µm-thick, high-quality nc-Si for micromorph solar cells [11]. Therefore, we deposited intrinsic nc-Si via plasma enhanced chemical vapour deposition (PECVD) on sample #3 in table 2. In figure 5 (a), a cross-section SEM of a 3 µm-thick nc-Si is shown. It is clear that no cracks are present at the interface. When a 5 µm-thick nc-Si is deposited (Figure 5 (b)), we notice cracks in nc-Si layer.

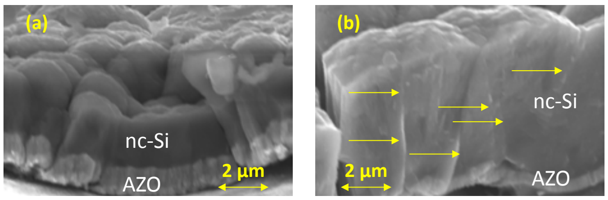

Figure 5 Cross sectional SEM of Al/AZO/nc-Si; (a) 3 µm-thick, (b) 5 µm-thick.

These results are coherent with the correlation length and rms roughness that have been found. Generally, the cracks appear when the thickness of nc-Si overcomes the so-called threshold thickness [17]. This parameter depends on aspect ratio of the structures. In order to evaluate the scattering properties of KOH-etched Al foils, we measured angular intensity diffraction (AID), displayed in figures 6. The samples shown here are etched with a concentration of 100 g/L and for t = 2 minutes. The temperature instead is varied from 35 to 70 °C.

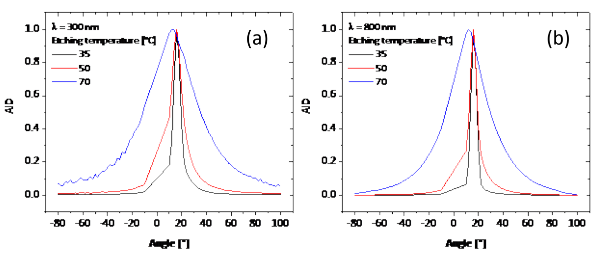

Figure 6 Normalized AID plots of KOH-etched samples ((a) λ= 300 nm and (b) λ = 800 nm) at a concentration of 100 g/L at different temperatures. The etching is done for 2 minutes.

It is clear how, by increasing the etching temperature, the angular scattering properties improve accordingly.

B. Etching of TCO sacrificial layer

In this approach, AZO sacrificial layer is deposited and then etched. As in the case of bare Al etching, the process is heavily dependent on temperature. Indeed, as SEM images are showing, the size of the craters is gradually increasing. This is also confirmed by AFM analysis shown in the figures 7 (b), (d), (f) and (h).

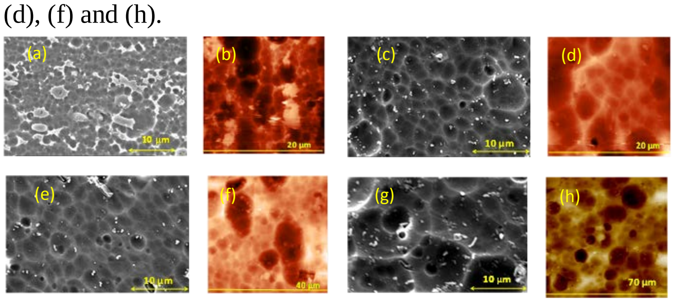

Figure 7 SEM and AFM of etched AZO layers at different temperatures; (a-b) T = 35 °C, (c-d) T = 50 °C, (e-f) T = 60 °C, (g-h) T = 70 °C.

By processing the AFM images, we calculated the correlation length and RMS roughness shown in the table below. Correlation length increases with etching temperature, while we did not find any trend in rms roughness.

Table 3 Parameters of KOH-etched AZO sacrificial layer

T [°C]	L_c [µm]	σ_{RMS} [nm]	L_c/σ_{RMS}
35	1.8	408	0.22
50	2.2	262	0.12
60	5.0	354	0.07
70	5.4	443	0.08

This might be due to the different way the craters are formed when different temperatures are employed. In this case the measured AID of the samples shows better angular scattering compared to the factory baseline texturing made by sodium hydroxide (NaOH), as figures 8 display.

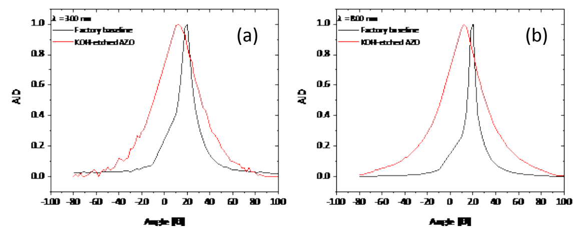

Figure 8 Normalized AID plots of KOH-etched sacrificial layer AZO ((a) λ= 300 nm and (b) λ = 300 nm) at 70°C for 2 minutes compared with standard, industrial baseline.

IV. Conclusions

We have explored a novel method to texture the temporary Al foil for thin-film, silicon-based, flexible solar cells. It consists of using potassium hydroxide. First, we mapped the etching rate and characterized the etching kinetics through Arrhenius model. Activation energy has found to be in the range of 0.5 eV. We obtained crater-like structure that are characterized with an aspect ratio of ~12% independently of the etching temperature. This allows to grow a 3 µm-thick layer of nc-Si without any defects. Angular scattering has been measured and found to be excellent from -40° to 40° when high etching temperature is employed. We developed also a method employing an AZO sacrificial layer (~600 nm-thick) etched in KOH that shows increasing 2D correlation length with etching temperature. These samples show excellent angular scattering compared to industrial baseline.

References

[1] A. V. Shah et. al., https://doi.org/10.1002/pip.533
[2] O Kluth, et.al., https://doi.org/10.1016/S0040-6090(99)00085-1.
[3] M. Berginski, et. al., https://doi.org/10.1016/j.tsf.2007.10.029.
[4] J. Müller et. al., Solar Energy, doi.org/10.1016/j.solener.2004.03.015.
[5] M. Kambe et al., doi: 10.1109/PVSC.2009.5411411.
[6] H. Sai et. al., Appl. Phys. Lett 101, 173901 (2012).
[7] J. Bailat *et al*., JAP 2003; 93: 5727–5732.
[8] Yoshiyuki Nasuno et al 2001 Jpn. J. Appl. Phys. 40 L303.
[9] Hongbo B.T.Li et. al., doi:10.1016/j.solmat.2008.11.013.
[10] H. Tan, et al, Appl Phys. Lett. 103, 173905 (2013)
[11] H.Tan et. al., doi: 10.1002/pip.
[12] T. Matsui T, et. al., Jpn J Appl Phys. 2015;54(8S1):08KB10. https://doi.org/10.7567/JJAP.54.08KB10
[13] K. Jaeger et al., https://doi.org/10.4229/28thEUPVSEC2013-3BO.5.5

[14] M.N.van den Donker, et. al. https://doi.org/10.1016/j.solmat.2006.11.012
[15] M. H Yun et. al., https://doi.org/10.1116/1.590282
[16] H. Seidel et. al., doi: 10.1149/1.2086277
[17] H. Sai et. al., https://doi.org/10.1063/1.346